Journal of Computational and Applied Mathematics 19 (1987) 243–259
North-Holland

Completeness of zero curve tracing for analytic functions

Dorothea A. KLIP
Department of Physiology and Biophysics, Department of Computer and Information Sciences, University of Alabama at Birmingham, Birmingham, AL 35294, U.S.A.

Received 10 April 1986
Revised 15 January 1987

Abstract: Empirical data for the polynomial confirm the efficiency of exploring function structure as a means of isolating the zeros of a scalar analytic function defined on a disk (Klip, 1985). In exceptional cases the tracing is not complete which means that certain arcs may not have been traced. A mathematical basis for the algorithm which investigates and restores completeness, the so-called completeness algorithm, is presented. The main theorem is that completeness of the tracing, as verified at the isolated zeros, is sufficient for completeness of the tracing. Its proof evolves along various lemmas, one of which provides a new condition for the location of the critical points. The paper concludes with a brief description of the completeness algorithm.

Keywords: Simultaneous zero isolation, zeros of analytic functions, polynomial solution, critical points, graphs and structure of analytic functions

Introduction

The search for the zeros of an analytic function as directed by the zero curves of its real part (r-arcs) and optionally those of its imaginary part (i-arcs) was applied to the complex polynomial and shown to be very efficient (Klip [6]). According to the Principle of the Argument, along the boundary of a disk $C := (0, R)$ which contains n zeros, the total increment of the function argument is $2\pi n$ (Ahlfors [1]). For the polynomial P of degree n this argument increment implies that the boundary of C is intersected alternatingly by arcs of $\mathrm{Re}(P) = u(x, y) = 0$ and arcs of $\mathrm{Im}(P) = v(x, y) = 0$, which results in a total number of $4n$ intersection points. Since ∞ is a pole of P, the arcs stretch to infinity under equal angles. As is seen from the outline of the Main Algorithm in Appendix A, these $4n$ intersection points are isolated and each of these isolating intervals serves as a basis for a triangular tracing procedure. Since the function is defined by its real part only (except for an imaginary constant), it is sufficient for zero finding to trace one kind of arcs. If only r-arcs are traced, $2n$ triangular pathways—starting at the boundary—are constructed, while taking care of triangular bisecting if the new vertex yields a function value located in a different halfplane (the triangle has then been intersected by an adjacent i-arc). The calculations are done in floating-point arithmetic and the program is designed such that precision can be adjusted locally up to a certain maximum defined by the

user. In the vicinity of a zero (which is an intersection point of an r- and an i-arc) the triangle size becomes very small and the tracing terminates if a preset break-off criterion for the stepsize is met.

Zero curves are piecewise Jordan arcs of steepest descent and therefore optimal among possible pathways. Stepsize is a measure for distance to the zero and thus for required precision. The self-correcting properties of curve tracing (see Klip [6]) allow stepsize as well as precision to be dynamically adjusted. A linear search for the zeros is much more efficient than the 2-dimensional approach of older search algorithms reviewed by Henrici [4] and Collins [3], as was demonstrated in Klip [6]. We want to mention the linear algorithm for root solving of polynomial equations, recently described in a sequence of papers by Renegar, the latest of which is [10]. The homotopy algorithm amounts to a triangulation of space. In comparison our algorithm may be considered a triangulation of zero curves. The expression for the computational complexity has the same order of magnitude as a function of n as our algorithm. Detailed comparison of the complexity will be given elsewhere. The homotopy algorithm does not have the advantages of zero curve tracing mentioned above. Also, in our algorithm multiple zeros do not present an impediment to efficiency, contrary to Renegar's approach and other algorithms for simultaneous zero isolation. Due to its analytic basis it naturally extends to analytic functions defined on a disk.

This paper concentrates on the perfection of the algebraic results, i.e. on the mathematical basis of the subalgorithm which provides automatic verification (followed by restoration) of completeness of the tracing. From a practical point of view the 'main algorithm' is self-contained by virtue of the graph option combined with the possibility to analyze any region separately (see [6]). The latter method is even profitable when in regions containing a multiple zero or a cluster greater maximal precision is required than at other locations. The 'completeness algorithm' effects the partition of C by the zero curve structure into regions of equal function quadrant. Its efficient design is based on the fact that completeness, if verified at the zeros, is sufficient to ensure completeness of the traced structure. This is formulated in Section 2 by Theorem 1. Certain properties of the zero curve structure which are easy to verify, will be simply mentioned in the form of statements. More complex issues which are basic to the proof of the main theorem are stated in Lemmas 1 through 5. In Section 3 a brief account of the completeness algorithm is given, but technical details will be presented in a subsequent paper. The term 'uniqueness' used in Klip [6] has been replaced by 'completeness' in order to avoid confusion with the 'uniqueness theorem' of analytic functions found in Markushevich [8].

Throughout the text it is assumed that sufficient precision for the calculations is available to meet the objectives of the investigation.

Outlines of the main algorithm and the completeness algorithm are given in Appendices A and B. A few examples of the traced structure can be found in Appendix C.

1. Properties of the zero curve configuration

General orientation

A zero curve is a chain of piecewise Jordan arcs. The only points of discontinuity are possible zeros of f' located on it. The concept of r-arc as it is referred to in the text is the following.

Definition 1. An *r-arc of an analytic function* $f(z) = u(z) + iv(z)$ is a Jordan arc with the equation $u(z(t)) = u(x(t), y(t)) = 0$ on an interval of t-values, such that in the open interval u'_x and u'_y do not vanish simultaneously. In addition the range of t-values is chosen such that the left endpoint $z(t_1)$ is either an intersection point of $u = 0$ with the boundary of C or a zero of f'. The right endpoint $z(t_2)$ is either a zero of f' (for which $f \neq 0$) or a simple or multiple zero of f.

With this restriction we can now state

Lemma 1. *A zero arc is a path of steepest descent.*

The proof is given in [6].

From the Taylor expansion of f at a zero z_0 of f' located on an r-arc it is seen that $2m$ r-arcs converge at z_0 under equal angles, where $m \geqslant 2$ is the multiplicity of z_0 as a zero of $g(z) := f(z) - iv(z_0)$. z_0 is referred to as *branch point* of the structure.

Definition 2. *A branch point of the zero curve structure*, briefly called *branch point* in this text, is an intersection point of r-arcs (or of i-arcs) in which $f \neq 0$.

The discontinuity of the arcs at possible branch points or multiple zeros is removable so that we can introduce the concept of branch. Although originally introduced for the polynomial, the local considerations hold for a general analytic function defined on a disk.

Definition 3. A branch of the zero curve structure of an analytic function defined on a disk is a chain of zero arcs, where discontinuity of $\arg(z'(t))$ at possible branch points or multiple zeros is removed by selecting for the continuation of γ_1 that arc γ_2 which fulfills

$$\lim_{t=t^*} \arg_{\gamma_2}(z'(t)) = \lim_{t=t^*} \arg_{\gamma_1}(z'(t)) + \pi \pmod{2\pi}.$$

Since the boundary of a disk C containing the zeros intersects the set of r-arcs (i-arcs) of a polynomial P of degree n in $2n$ distinct points, one may conclude:

Lemma 2. *The zero curve structure of a polynomial of degree n consists of n r-branches and n i-branches.*

Some branches may contain more than one zero, so that in this case there are branches which do not contain zeros. As an example we refer to Appendix C, Fig. 7, a polynomial with real roots only. For real polynomials the x-axis is an i-branch and an axis of symmetry. Since in this case all zeros are real, one i-branch (the x-axis) contains all zeros, so that the remaining $n-1$ i-branches do not contain a zero. They intersect the x-axis in a branch point, which is a zero of f'. Figures 7 and 8 of Appendix C are more extensively discussed below.

With respect to 'the function f analytic on a disk', briefly referred to as f, we remark

(1) the boundary ∂C cannot be part of an r- or i-arc,

(2) if f contains n zeros in C, ∂C may be intersected by more than $4n$ r- and i-segments. The number of intersection points is finite, because an infinite number would imply a limit point of the set $\{z_1, \ldots\} \in \partial C$ for which $u = 0$, from which it follows $\mathrm{Re}(f) = 0$ identically, so that $f = c$ (c an imaginary constant). In case of the polynomial P, when scanning ∂C at regular intervals, the stepsize can be adjusted such that each interval of sequential points contains one intersection

point with a zero arc. The isolation of the $4n$ intersection points can be achieved, starting with any stepsize s, but it is profitable to choose $\pi R/2n$ as basic value for s if the centroid of the zeros is in the origin.

In general there will not be a simple way to know the number of zeros of f in C. Also, using an arbitrary stepsize, one may miss a descending arc, because 2 successive r-arcs may belong to the same branch and give a total quadrant increment 0. Moreover, the algorithm cannot distinguish between an increment -1 and 3. At this time we will not pursue an investigation of the ability of the tracing algorithm to find all zeros of f in C. It is obvious that for f the main algorithm should include monitoring the position of each tracepoint relative to C (and abandon the tracing if it is outside C), since arcs of descent may lead to roots outside C. A precise analysis of the structure for f based on its order and the location of its zeros relative to ∂C has still to be provided. However, due to the orthogonality of the converging arcs at each simple zero it is unlikely that the chosen stepsize is critical for a successful tracing of the structure. We state:

Conjecture. *The main algorithm combined with the completeness algorithm applied to a function analytic on a disk C will lead to successful tracing of its zero curve structure, provided no zeros are located on the boundary* ∂C.

Univalent and multivalent regions

The zero curve structure provides a partitioning of C into open regions relative to the boundary of C, i.e. each region contains at least one boundary segment. The polynomial function P is univalent or 'schlicht' in the open regions whose boundary contains one boundary segment of C. There is a 1-1 correspondence between the points in such a region and their image in the w-plane, which constitutes one quadrant. The remaining regions contain more than one boundary segment. It is obvious that the mapping is not 1-1. They form the multiple inverse image of one quadrant in the function plane. For later reference we define:

Definition 4. A branch region B is a region in C in which u and v do not change sign and whose boundary contains more than one boundary segment of C. As its order we define the number of boundary segments it contains.

The branch regions are the only possible locations of those zeros of P' which are not part of the structure itself. In the absence of branch points a branch region is bounded by an equal number of boundary segments, r-arcs and i-arcs. We referred above to Appendix C, Fig. 7 in which the structure of the so-called 'Wilkinson's polynomial' is displayed, by means of tracepoints generated with our program. In Wilkinson [11] the instability was discussed of this polynomial in which all zeros are equally spaced. A very small change in the coefficients brings about a large shift of the larger zeros to the complex plane. The effect on the zero curve structure as a result of a small perturbation in the coefficient of z^{19} is shown in Fig. 8 of Appendix C. The structure of the unperturbed polynomial consists merely of univalent regions, consistent with the fact that all zeros of the derivative are branch points. In Fig. 8 one discerns a branch point of r-arcs in each halfplane and two branch regions of order 3, indicated by I and II. The ability to partition C into univalent regions will play an important role when approaching the problem of solving a small system of non-linear equations on an analytical basis.

Incompleteness of the tracing

We want to impose the condition that the zero curve configuration is completely covered by the triangular pathways. Pathways of traced r-arcs which bound the same branch region may intersect. They will intersect when approaching a branch point. Continuation of the tracing beyond a domain of adjacent or intersecting r-arcs depends on the geometric configuration of the tracing triangle and the converging arcs and is essentially a matter of chance. Thus it may happen that parts of arcs are multiply traced, while other segments are not traced. In Appendix C, Fig. 9 an example is given of a complex polynomial where one arc is not traced. This case is also discussed in [6]. In itself this will rarely be a cause of failure to isolate some zeros, since in general each zero is approached by at least one arc which bounds two contiguous univalent regions, so that an intersection of traced pathways cannot occur.

The important contention is that completeness of the traced structure can be checked at the isolated zeros, i.e. distinctness of the pathways at the zeros implies completeness of the pathways.

2. Main theorem of completeness of tracing

The proof of Theorem 1 is based on the fact that 2 pathways of traced r-arcs (i-arcs) intersect at most once (Lemma 5). In this connection we have to look at the structure at the site of locally converging r-arcs in more detail. First, we show that a branch region contains at least one zero of f' (Lemma 3). Next, we show (Lemma 4) that the discrete tracing cannot cause a step-over to a different branch region due to an unnoticed intersection with i-arcs. One thus concludes that the branch points and the branch regions are the only sites where a coincidence of pathways can be initiated. These two lemmas are basic to the proof of Lemma 5.

We prove that a zero of f' is located in a branch region B. In Fig. 1 a region D' is sketched, whose boundary is a Jordan curve, which is intersected by 2 r-arcs α and α'. We suppose that D'

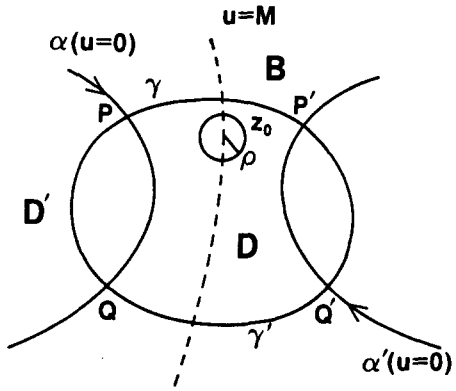

Fig. 1. The region D' is intersected by r-arcs α and α'. B is the branch region in part bounded by α and α'. Suppose that the boundary segment γ of $D := D' \cap B$ is intersected by distinct level arcs $u = c$. Let $c > 0$. Then, if ρ is small enough, $u < M$ along $\partial\Delta$, where $\Delta := (z_0, \rho)$. Equality only holds in the 2 intersection points with $u = M$. The Theorem of the Mean for harmonic functions is thus violated for Δ.

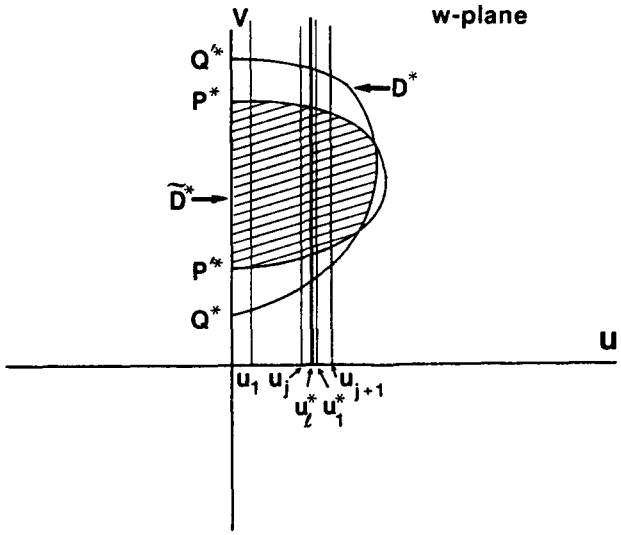

Fig. 2. According to the conformal mapping properties each point of the marked subregion $\tilde{D}^*$ of D^* in the w-plane is taken twice in D. There is a subregion D_j^* of $\tilde{D}^*$ bounded by $u = 0$ and $u = u_j$ which has disjoint inverse images in D, whereas the inverse images of the region D_{j+1}^* bounded by $u = 0$ and $u = u_{j+1}$ are not disjoint. According to Lemma 3 one can find $u = u_j^*$ whose inverse image consists of 2 intersecting u-level arcs in the branch region B.

is not intersected by i-arcs so that the region bounded in part by α and α' is a branch region B. Let $D := D' \cap B$ and let γ be one of the boundary segments of D. γ cannot be intersected exactly once by all u-level arcs of the set $\{u = c \mid c > 0\}$ which cover D. Because if all u-level arcs which intersect γ would be distinct, there would be an arc with maximum value $u = M$. One then could construct a circle $\Delta := (z_0, \rho)$ centered on $u = M$ and choose its radius ρ small enough so that $u < M$ everywhere along its boundary except in the intersection points with $u = M$. This leads to $M = u(z_0) > \int_{\partial\Delta} u(z)\, dz$, contrary to the Theorem of the Mean for harmonic functions.

We show that γ is intersected by a pair of u-level arcs, which intersect in a zero of f'. In case the segments of α and α' which bound D do not have an interval of v-values in common, one may extend D along one of the arcs to include such an interval, since an r-arc is a path of steepest descent. The possible inclusion of branch points in this extension does not alter the main argumentation. It is also no restriction to assume that each point of the image D^* of D in the w-plane cannot be taken more than twice in D. Taking into account that open sets are mapped onto open sets [8], under these assumptions the image D^* has a structure as sketched in Fig. 2. On the basis of the Argument Principle [1] it is seen that each point of the inverse image of the region $\tilde{D}^*$ bounded in part by the segment $P^*P'^*$ is taken twice in D. With respect to u-level arcs this implies that D is intersected by pairs of arcs which have the same u-value. We show that there is a limit point, i.e. not all pairs can be distinct. Each point on the segment $P^*P'^*$ in the w-plane is taken once on α and on α'. Due to the continuity of each analytic branch of the inverse function $z := f^{-1}(w)$ there is a value $u_1 > 0$ such that the subregion $\tilde{D}_1^*$ of $\tilde{D}^*$ bounded by $u = 0$, $u = u_1$ is mapped on 2 disjoint regions in D. By continuing the process of partitioning $\tilde{D}^*$ by equally spaced rectilinears $u = u_2, \ldots$ one must encounter a subregion $\tilde{D}_{j+1}^*$ of $\tilde{D}^*$, bounded by $u = 0$ and $u = u_{j+1}$ such that its inverse image does not map on disjoint regions in D. However, since $\tilde{D}_j^*$ does map on disjoint regions $D_j^{(1)}$ and $D_j^{(2)}$, the boundary line $u = u_j$

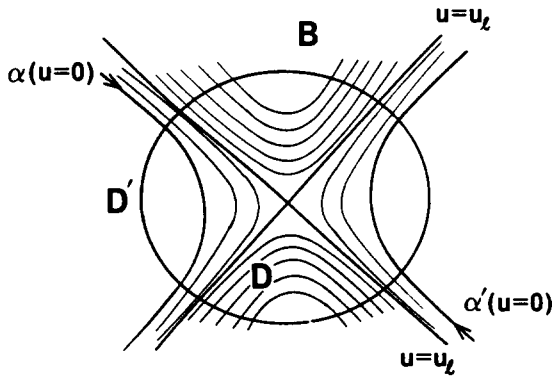

Fig. 3. The set of u-level arcs in D is sketched. The pair $u = u_l$ intersects orthogonally in a simple zero of f'.

maps on 2 distinct u-level arcs in D, unless $u = u_j$ is the least upperbound of the boundary lines of the regions whose inverse images are disjoint.

We proceed to construct the least upperbound by means of the process of bisection and define $u_1^* = \frac{1}{2}(u_j + u_{j+1})$ so that $u = u_1^*$ divides $E_1^* := \tilde{D}_j^* \cap \tilde{D}_{j+1}^*$ into 2 regions $E_{1,1}^*$ and $E_{1,2}^*$. Let $E_{1,1}^*$ be the subregion closest to the v-axis whose inverse images in D are not disjoint and define $E_2^* := E_{1,1}^*$. Let $u = u_2^*$ divide E_2^* into 2 regions of equal width, etc. The width of the subdivisions E_k^* thus obtained tends to 0, so that the sequence $u_1^*, \ldots$ tends to the limit u_l^*. The inverse images of $u = u_l^*$ are 2 u-level arcs, with the property that they cannot be disjoint, because in this case one could find $\epsilon > 0$, such that the region bounded by $u = u_l^*$ and $u = u_l^* + \epsilon$ projects onto two disjoint regions, contrary to the assumption that each region $\subset \tilde{D}^*$ to the right of $u = u_l^*$ does not map onto disjoint regions. Consequently, the inverse images of $u = u_l^*$ are 2 intersecting u-level arcs, whose intersection point z_0 is a zero of f'. Earlier investigation of the structure at a zero of f' (see Section 1) accounts for the configuration sketched in Fig. 3. We have proven:

Lemma 3. *If 2 r-arcs intersect a region, whose image is contained in the upper (lower) halfplane, then the branch region bounded in part by these arcs contains at least one zero of f'.*

Since Lemma 3 holds for i-arcs as well, one may more formally state

Corollary 1. *A zero of f' is located in the intersection $D := D_1 \cap D_2$, where $D_k := \cup\{ D_{j,k} \mid k = 1, 2;$ $D_{j,k} := D'_{j,k} \cap B\}$. $D_{j,k}$ is any region, whose image is contained in one halfplane, which is intersected by at least 2 r-arcs ($k = 1$) or i-arcs ($k = 2$) which bound B.*

In Figs. 8 and 9 of Appendix C a sketch is made of the location of the critical points, which in these examples are simple zeros of f'. Therefore they are found as the intersection points of one u-level and one v-level arc. These levels arcs intersect the converging i-arcs respectively r-arcs orthogonally. Due to the continued interest in the location of the critical points, e.g. see Marden [7], this result is of broader interest.

It was mentioned in the introduction that a step-over to the other halfplane as shown by a third quadrant at the new tracepoint, induces reduction of the tracing triangle. We want to investigate now if the traced pathway could be affected by an unnoticed intersection with arcs of

the other kind. This means that we study the structure on the macrolevel, with the assumption that the sides of the triangle for an r-arc are intersected an even number of times by i-arcs. We prove:

Lemma 4. *An unnoticed intersection of a tracing triangle of an r-arc α by i-arcs does not affect the traced pathway.*

Proof. Let T be the first triangle of the traced pathway of an r-arc α which is intersected by i-arcs and let its base b be the side where α enters. By virtue of the definition of T only its remaining sides can be intersected by i-arcs. Let T^* be the next tracing triangle as defined by the exiting r-arc and let $S := T \cup T^*$. In general there will be just one i-arc β whose intersection with T is unnoticed and β will intersect α in a zero of f, as shown in Fig. 4. The 'main algorithm' discovers at V_3^* a quadrant different from those at V_1 and V_2, so that bisecting is undertaken (Step 4). It is likely that an 'inconsistency' is found (Step 4a), since at V_2^* a quadrant q_1 or q_2 is expected. Backstepping combined with bisecting will eventually lead to the isolation of the zero. The situation as sketched in Fig. 4 *must* hold if all u-level arcs in S are distinct. Since α is one of them, α intersects β, due to the orthogonality of the two kinds of level arcs.

We therefore consider the case that not all u-level arcs in S have distinct values. Since β is an arc of descent, the u-level arcs which intersect β do have distinct values. Therefore there must be at least one pair of arcs which intersects in a zero z_0 of f'. The set $s:\{u(z_0)\}$ of intersecting u-level arcs divides the region into sectors in which either $u > u(z_0)$ or $u < u(z_0)$. Suppose $u(z_0) > 0$. Then α is located in a sector in which $u < u(z_0)$. This implies that z_0 is located in the

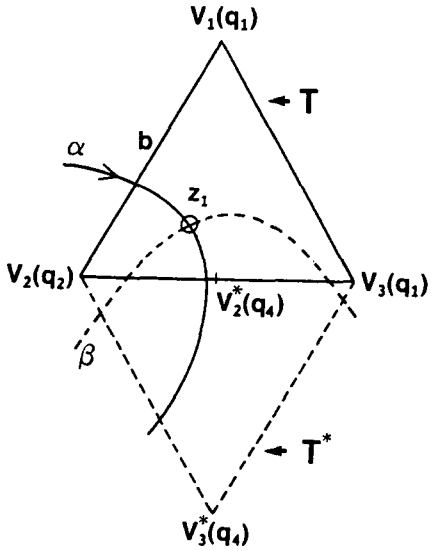

Fig. 4. The traced r-arc α enters T at its base b. The intersection with i-arc β is not detected in V_3 because β intersects one side of T twice. If the level arcs of both kinds in T are distinct, α intersects β due to the orthogonality of the 2 kinds of arcs. The Main Algorithm finds an inconsistency at V_2^* but proceeds (Step 4a, Appendix A) towards the isolation of zero z_1.

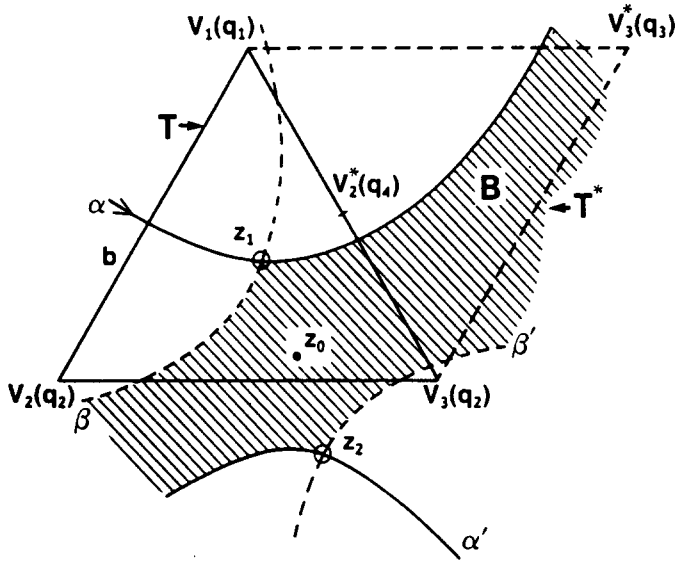

Fig. 5. In the presence of a critical point z_0 in the branch region bounded in part by α and β the position of the arcs can be described relative to the structure generated by z_0. The case is sketched that T is intersected (unnoticedly) by arcs β and β'. In the next step a third quadrant is found at V_3*. The Main Algorithm eventually isolates z_1.

branch region in part bounded by α and β. At the same time this sector cannot be intersected by β since we study the case that the arcs do not intersect. With just one arc β which intersects T, in the next step β is 'bypassed', which means that this intersection does not affect the traced pathway. Suppose now that there is another arc β' which intersects T. Then, if z_0 is the only critical point in the branch region specified by the 3 arcs and if it is a simple zero of f', α must intersect β', since there are only 2 sectors in which an i-arc can be located. Consequently, β is intersected by α', the counterpart of α with respect to z_0. This case is shown in Figs. 5 and 6. At z_0 one may write $f(z) = f(z_0) + (z - z)^2 h(z)$ $(h(z_0) \neq 0)$ from which it follows that the 4 arcs form approximately a mutually orthogonal set of orthogonal hyperbolas: $(x - x_0)^2 - (y - y_0)^2 = c \cos \gamma$ respectively $2(x - x_0)(y - y_0) = c \sin \gamma$ (c a real constant). In both cases a third quadrant is found at V_3* and the 'main algorithm' takes proper action. In Fig. 5 'inconsistency' is found at bisecting, so that the previous triangle base b is bisected and eventually z_1 is isolated. In Fig. 6 the case is sketched that T is intersected by the other r-arc α' which belongs to the structure generated by z_0. In this case a 'step-over' takes place and the neighboring zero z_2 is isolated by the algorithm.

Finally, if α does not intersect either of the i-arcs, then z_0 is either a multiple zero of f' or there is another critical point in the branch region defined by this set of arcs. If in this case the side of continuation is intersected by β then the unnoticed intersection is discovered in the next step and on the basis of the bisecting feature the algorithm will yield a tracing triangle for α which is not intersected by i-arcs. The branch region bounded by the arcs must then have at least order 3. This case can be studied in Fig. 9 of Appendix C. We have thus analyzed the structure on the macrolevel. □

The result can be expressed as follows.

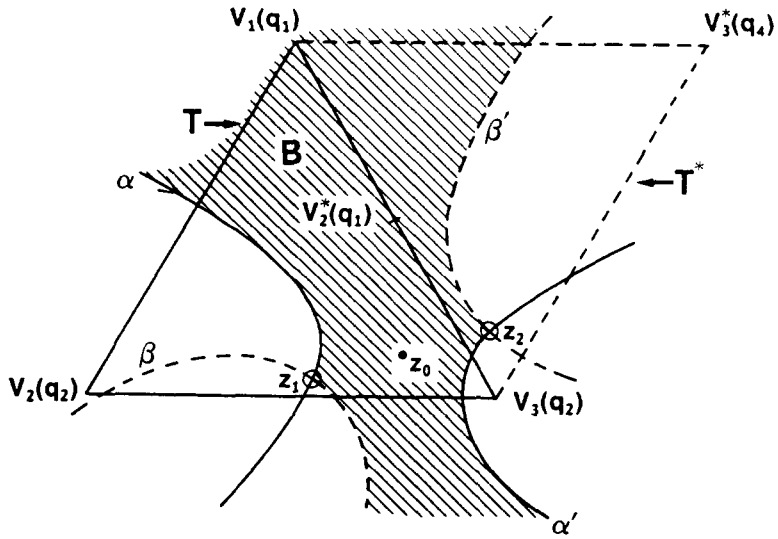

Fig. 6. In a slightly different orientation of T relative to the structure, T is intersected by a second r-arc α', which leads to a step-over to this arc and the isolation of zero z_2.

Corollary 2. *Each terminated pathway of traced r-arcs (i-arcs) is contained in one open halfplane, except perhaps for an incidental and inconsequential intersection with an i-arc.*

The last intermediate result is the following:

Lemma 5. *Two pathways S_1 and S_2 of traced r-arcs can intersect only once.*

Proof. The proof is given by contradiction. Suppose that there are two distinct sites of intersection, Ω_1 and Ω_2. According to Corollary 2, the images of S_1 and S_2 can be considered to be contained in one halfplane. The distinctness of the regions Ω_1 and Ω_2 implies that there are segments α_1 and α_2 on the respective traced arcs which are covered by just one pathway. Since Ω_1 and Ω_2 are distinct regions, being the intersection of pairs of distinct tracing triangles, it follows from Lemma 3 that each—possibly after extension—contains a zero of f', z_1^* respectively z_2^*. One may then consider the closed curve γ which outside Ω_1 and Ω_2 coincides with the distinct arcs α_1 and α_2 and inside Ω_1 and Ω_2 with the level arcs $v_1 = v(z_1^*)$ respectively $v_2 = v(z_2^*)$, which intersect α_1 and α_2 orthogonally. We apply to γ a theorem named after Riemann [50, p. 156].

$$\int_\gamma u\,\mathrm{d}v = \int_\gamma u\frac{\partial v}{\partial x}\,\mathrm{d}x + u\frac{\partial v}{\partial y}\,\mathrm{d}y = \int\int_G \left(\left(\frac{\partial u}{\partial x}\right)^2 + \left(\frac{\partial u}{\partial y}\right)^2\right)\mathrm{d}x\,\mathrm{d}y$$

$$= \int\int_G |f'|^2\,\mathrm{d}x\,\mathrm{d}y > 0.$$

In the derivation Green's theorem has been applied. G is the region enclosed by γ. However, γ consists of the arcs α_1 and α_2 along which u vanishes, and the level arcs v_1 and v_2 along which $\mathrm{d}v$ vanishes. Therefore $\int_\gamma u\,\mathrm{d}v = 0$, which can only be true if f is constant. □

We are now prepared to prove that if the terminal pathways are distinct, the structure has been completely traced. Distinctness of the terminal r-pathways can be verified by establishing the sector in which they are located, as defined by the converging i-arcs at each zero (see Step I of the Completeness Algorithm, Appendix B).

Theorem 1. *The tracing of the zero curve structure is complete if and only if the tracing, as verified at the isolated roots, is complete.*

Proof. Since for the polynomial the number of r-arcs intersecting the boundary of the root enclosing disk C is known in advance, completeness of the tracing as expressed by distinctness of the terminal pathways, implies completeness of the traced structure. For the general function one should in addition verify that all terminal arcs at each zero have been traced. The necessity of the condition is self-evident. We prove the sufficiency relative to the traced r-arcs, and notice on the basis of Corollary 2 that only one branch region B needs to be considered. The proposition implies that there is a site of step-over Ω_1. Let S_1 and S_2 be the corresponding traced pathways, so that $\Omega_1 := S_1 \cap S_2 \neq \emptyset$. It is no restriction to assume that the pathways of traced r-arcs entering Ω_1 are all disjoint, because otherwise one can follow from Ω_1 a pair of coinciding pathways in upward direction (increasing $|v|$-values) until an earlier incident of a step-over. Of course, such backstepping terminates, since $|v|$ attains its maximal value at the boundary and each arc is initially singly traced. Due to the supposed step-over of one of the entering pathways at Ω_1, at least one descending arc β_1, emanating from Ω_1, is not traced. If β_1 terminates at a root, the proposition is proven. We thus suppose that β_1 enters a different site Ω_2 of intersecting pathways. If the entering pathways are disjoint, there is at least one exiting arc at Ω_2 which is not traced, since β_1 is an entering arc for Ω_2. We therefore suppose that some of the entering pathways at Ω_2 trace the same arc, so that it may happen that as a result of a step-over at Ω_2 all exiting arcs are traced. We again follow a pair of coinciding pathways upwards until the site Ω_3 is reached where the entering arcs are singly traced. It is noticed that $\Omega_1 \cap \Omega_3 = \emptyset$, since a closed configuration of pathways and traced arcs cannot occur (Lemma 5). The number of distinct regions $\Omega_1, \Omega_2, \ldots$ is finite, since it cannot exceed the number of zeros of f'. Therefore the argument can only be repeated a finite number of times, so that there must be a descending arc β_2 which is not traced and whose right endpoint is a zero of f. □

3. The completeness algorithm

The algorithm Separate-Paths (Appendix B) starts with investigation of the completeness. Under the completeness option Steps 5a and 7 of the Main Algorithm (Appendix A) are executed. The high-order iteration procedure

$$z_{n+1} = z_n + \phi_k(z_n), \quad k = 2, 3, \ldots \quad \text{with } \phi_k(z) = (k-1)\frac{(f'/f)^{(k-2)}}{(f'/f)^{(k-1)}} \tag{1}$$

(Pomentale [9]) appeared most appropriate for our purposes. Its order of convergence k is independent of the multiplicity of the zero, which is important in view of the applicability of the Main Algorithm to functions which have multiple zeros. Since the algorithm may most fre-

quently be applied to the polynomial, another important consideration for this choice was Pomentale's contention that in this case (1) is most efficient for $k = 4$ if $n > 4$. Neither property holds for the more popular Laguerre iteration function.

In the next step the orientation γ of the zero curve configuration at zero ρ is defined by $-\arg(f^{(m)}(\rho))/m$, where m is the multiplicity of ρ. This choice for γ is consistent with the expression for the angles of the tangent lines at ρ, derived by Klip [6], $\{\phi(k) = -\alpha + k\pi/2m \mid k = 0, \ldots, 4m-1;\ f = (z-\rho)^m h(z);\ \alpha = \arg(h(\rho))/m\}$, so that $\gamma = -\alpha$. The angles of the entering r-pathways are defined by associating these pathways with the sectors in which the converging i-arcs divide the region at ρ (Step I of Completeness Algorithm, Appendix B). According to Theorem 1, if at each zero the pathways terminate in distinct sectors, completeness of the tracing occurred (Step II, Appendix B). Otherwise pairs of arcs with coinciding terminal pathways are simultaneously retraced. The algorithm rapidly identifies the site of intersection and locates a pair of triangles of each pathway to which the following lemma applies.

Lemma 6. *Let $T_{1,i}$ respectively $T_{2,j}$ be tracing triangles for arcs α_1 and α_2 and let I_1 and I_2 be the corresponding intervals of $|v|$-values. If $T_{1,i} \cap T_{2,j} = \emptyset$ and $I_1 \cap I_2 \neq \emptyset$, then the partial pathways $S_1 = \sum_{k=1}^{i} T_{1,k}$, $S_2 = \sum_{k=1}^{j} T_{2,k}$ cover distinct arcs.*

Proof. If the contention is false, then S_1 and S_2 partially cover the same arc, say α_1. This is also true for the last triangles $T_{1,i}$, $T_{2,j}$ in each chain, since pathways S_1 and S_2 can intersect only once (Lemma 5). Since $T_{1,i} \cap T_{1,j} = \emptyset$, distinct segments of α_1 are covered and since $|v|$-values strictly decrease, $I_1 \cap I_2 = \emptyset$, contrary to the assumption. □

By means of the process of bisection and advancing with the smaller triangle size, while calculating the new $|v|$-interval, one generates a sequence of subtriangles $T_1^{(s)}$, $T_2^{(s)}$, to which Lemma 6 can be applied. The last pair of large triangles $T_{1,i}$, $T_{2,j}$ is advanced according to the location of the new tracepoint of each $T^{(s)}$ sequence. There are 2 possibilities. The bisection procedure may lead to a triangle size which satisfies the condition for break-off. This implies that high-order iteration to the approached zero z_0 of f' is expected to be successful. From the orientation of the structure of $g(z) := f(z) - iv(z_0)$ at z_0 the direction of continuation of the r-arcs beyond z_0 can be derived. Subsequently a choice of continuation for one of the pathways is made. The other possibility is that the advancing process with smaller stepsize, which of course induces a reorientation of one of the large triangle chains, leads to separation of these chains. The administration process is effectively achieved by means of Klip [5]. Details will be provided elsewhere.

Acknowledgement

I would like to express my special thanks to Joyce Iannuzzi, who through the years has assisted me very efrficiently in solving any systems related problem. Thanks are also due to Frances Roland, whose careful design of the figures will have contributed to clarifying the text. Douglas McLean was so kind to produce the graphs from my data by means of an IBM 7372 plotter.

References

[1] L.V. Ahlfors, *Complex Analysis* (McGraw-Hill, New York, 1966).
[2] C. Carathéodory, *Funktionentheorie I* (Birkhäuser, Basel, 1950).
[3] G.E. Collins, Infallible Calculations of Polynomial Zeros, in: J.R. Rice, Ed., *Mathematical Software III* (Academic Press, New York, 1977) 33–68.
[4] P. Henrici, *Applied and Computational Complex Analysis I* (Wiley, New York, 1974).
[5] D.A. Klip, The variable cell-length listprocessor VARLIST, in: *Proc. ACM Annual Conference* (Association for Computing Machinery, New York, 1974) 128–132.
[6] D.A. Klip, Isolation of the zeros of a complex polynomial by exploring function structure, in: V. Lakshmikantham, Ed., *Trends in the Theory and Practice of Non-Linear Analysis* (North-Holland, Amsterdam, 1985) 207–215.
[7] M. Marden, The search for a Rolle's theorem in the complex domain, *Amer. Math. Monthly* **8** (9) (1985) 643–650.
[8] A.I. Markushevich, *The Theory of Analytic Functions: A Brief Course* (Mir, Moscow, English translation, 1983).
[9] T. Pomentale, A class of iteration methods for holomorphic functions, *Numer. Math.* **18** (1971) 193–203.
[10] J. Renegar, On the efficiency of a piecewise linear homotopy algorithm in approximating all zeros of a system of complex polynomials, *Math. Programming* (1985) preprint.
[11] J.H. Wilkinson, *The Algebraic Eigenvalue Problem* (Oxford University Press, London, 1965).

Appendix A

Procedure: Zero Isolation—Main Algorithm

Step 1: initialization:

isolate $4n$ intersection points of branches with C by calculating quadrant of f at division points W_j.

for polynomial P of degree n calculate rootbound R; disk $C := (0, R)$;
for $j = 1$ to $4n$ do; find $W_j \in \partial C$ such that $\{q_j \mid q_j = \text{quadr}(f(W_j))\}$ satisfy $q_{j+1} - q_j = 1 \pmod 4$; end;

Step 2: next arc (or next r-arc if only r-arcs are traced) is defined by start points W_j, W_{j+1}.

next-arc:
for $j = 1$ to $4n$ by 1 (or by 2) do; $V_1 := W_j$; $V_2 := W_{j+1}$; $q_1 := q_j$; $q_2 := q_{j+1}$;

Step 3: iterative tracing process: construct equilateral triangle V_1, V_2, V_3. Continuation is simply achieved by reflection.

next-tri:
$V_3 = e^{i\pi/3}V_1 + e^{-i\pi/3}V_2$; goto calc;
reflect:
if $q_3 = q_2$ then $V_3 := V_3 + V_1 - V_2$;
if $q_3 = q_1$ then $V_3 := V_3 + V_2 - V_1$;
calc:
$q_3 := \text{quadr}(f(V_3))$;
if $q_3 = q_1$ or $q_3 = q_2$ then goto reflect;

Step 4: since a different quadrant is found, triangle base V_1V_2 is bisected

bisect:
$V_m := (V_1 + V_2)/2$; $q_m := \text{quadr}(f(V_m))$;
if $q_m = q_1$ then $V_1 := V_m$; if $q_m = q_2$ then $V_2 := V_m$;
if $q_m = q_1$ or $q_m = q_2$ then goto check-break-off;

Step 4a: an unnoticed intersection with arcs of the other kind has occurred. Pick up vertices of previous triangle and bisect. Check on given break-off criterion.

inconsistency:
$V_j := \text{Prev}(V_j)$ $(j = 1 \text{ to } 3)$;
goto bisect;
check-break-off:
if $|V_1V_2| > \epsilon$ then goto next-tri;

Step 5: terminate tracing. Approximation V to zero is center of triangle prior to bisecting.

approx:
$V_j' := \text{Prev}(V_j)$ $(j = 1 \text{ to } 3)$;
$V := (V_1' + V_2' + V_3')/3$;

Step 5a: (optional) terminal point V_τ (for r-arc) is found from last triangle base.

term-point:
$V_\tau = 0.5*(V_1 + V_2)$;
if $|\text{Re}(f(V_\tau))/\text{Im}(f(V_\tau))| > \epsilon$ then do;
$V_1 := V_\tau$; if quadr $(f(V_\tau)) = q_2$ then $V_2 := V_\tau$;
goto term-point; end;
end next-arc;

Step 6: approximations are separated into sets of approximations to same zero on the basis of 'closeness': $|(r_i - r_j)/r_j| \leqslant 1/4\delta$ and 'remoteness': $|(r_i - r_j)/r_j| > 3/4\delta$.

analyze-results:
form $\{S_j \mid j = 1 \text{ to } t\}$;
$S_j := \{\text{Approx}(\text{zero}(j))\}$;
$\text{zero}(j) := \text{mean}\{S_j\}$

Step 7: (optional) refine zero(j) to desired accuracy by applying Pomentale's high-order iteration function.

refine: for $j = 1$ to t do;
call POMENT(P, zero(j)); find multiplicity m_j; end;

Step 8: (optional) under graph option certain trace points are plotted.

graph:
call DISPLAY;
end ZERO-ISOLATION;

(Outline of Main Algorithm)

Appendix B

Procedure: Separate-Paths—Completeness Algorithm

Step I. Administration of pathways. Steps 5a and 7 of Main Algorithm have to be executed. For each isolated zero r_j find orientation γ of set of i-arcs. For the μ terminal points V_τ of r-arcs $\{\alpha\}$ find sector number s by calculating vector r_jV_τ. Orientation γ and set of arcs $\{\alpha\}$ with sector number s are registered for zero r_j.

$P = \prod_{j=1}^{t}(z - r_j)^{m_j}$;
(*Subscript j is omitted in Steps I and II*)
for $j = 1$ to t do; $\gamma = -\arg(P^{(m)}(r))/m$;
for $k = 1$ to μ do;
$\beta = \arg(\overline{rV_\tau}) - \gamma$; $s_k = \beta/(\pi/m)$; end;
create file(r, γ, $\{\alpha, s\}$); end;

Step II. Check on completeness is iteratively executed (see return from Step IV. termin-1). In case of completeness both conditions $m = 2\mu$ and $s_k \neq s_{k'}$ $(k \neq k';\ k,\ k' \in \{1, \ldots, \mu\})$ hold at each zero.

check-compl: for $j = 1$ to t do;
for $k = 1$ to $\mu - 1$ do; for $k' = k + 1$ to μ do;
if $s_k = s_{k'}$ then goto separation; end;
end; end;
call EXIT;

Step III. Separation of pathways. By simultaneously tracing α_1 and α_2 relative to $|v|$ values one encounters triangles $T_{1,i}$, $T_{2,j}$ which are disjoint, while intervals of v-values do intersect. Intervals are determined by calculating intersection points of arcs α_1 and α_2 with T_1 and T_2. Subtracing is performed such that subtriangles are disjoint. For each generated subtriangle the $|v|$ value of traced arc at exit is generated. Advance large triangle or modify pathway.

separation:
$I_k := |v(\alpha_{k,\text{entr}})| > |v(\alpha_k)| > |v(\alpha_{k,\text{exit}})|$
$(k = 1, 2)$;
$T_{1,i} \cap T_{2,j} = \emptyset$; $I_1 \cap I_2 \neq \emptyset$;
rename:
$T_1 := T_{1,i}$; $T_2 := T_{2,j}$;
$v_1 := v(\alpha_{1,\text{exit}})$; $v_2 := v(\alpha_{2,\text{exit}})$;
init-subdiv:
$T_k^{(s)} := T_k$ $(k = 1, 2)$;
iter-separ:
if $T_1^{(s)} \cap T_2^{(s)} \neq \emptyset$ then do;
call BISECT$(T_1^{(s)}, T_2^{(s)}, |v_1|, |v_2|)$;
goto check-termin; end;
$k = 1$; if $|v_1| < |v_2|$ then $k = 2$;
ADVANCE $(T_k^{(s)})$;
check-tri:
$z_k := \alpha_{k,\text{exit}}$; if $z_k \in T_k$ then
goto iter-separ; $T_k :=$ ADVANCE(T_k);
if $z_k \notin T_k$ then
modify: $T_k :=$ ADJACENT(T_k, z_k);

Step IV. Termination. Calculate distance between tracepoints. Subtrating is continued if large triangles are not disjoint.

Continue tracing arc whose pathway was modified, according to Main Algorithm.

Isolate branch point b by high-order iteration applied to derivative P'. At b the attributes listed in Step I, which define structure, have to be calculated for $P_b := P - iv(b)$.

(Outline of Completeness Algorithm)

check-termin:
$z_k := \alpha_{k,\text{exit}}$ $(k = 1, 2)$;
if $|z_1 - z_2| \leqslant \epsilon$ then goto termin-2;
if $T_1 \cap T_2 \neq \emptyset$ then goto iter-separ; else
termin-1:
do; $k = 1$; if MODIF(T_2) then $k = 2$;
call CONTINUE(T_k); goto check-compl;
end;
termin-2:
$b := z_1$; call POMENT(P', b);
create file$(b, \gamma, \{\alpha, s_k\})$;
register s_k (exit) $(k = 1, 2)$;
goto termin-1;
end SEPARATE-PATHS;

Appendix C

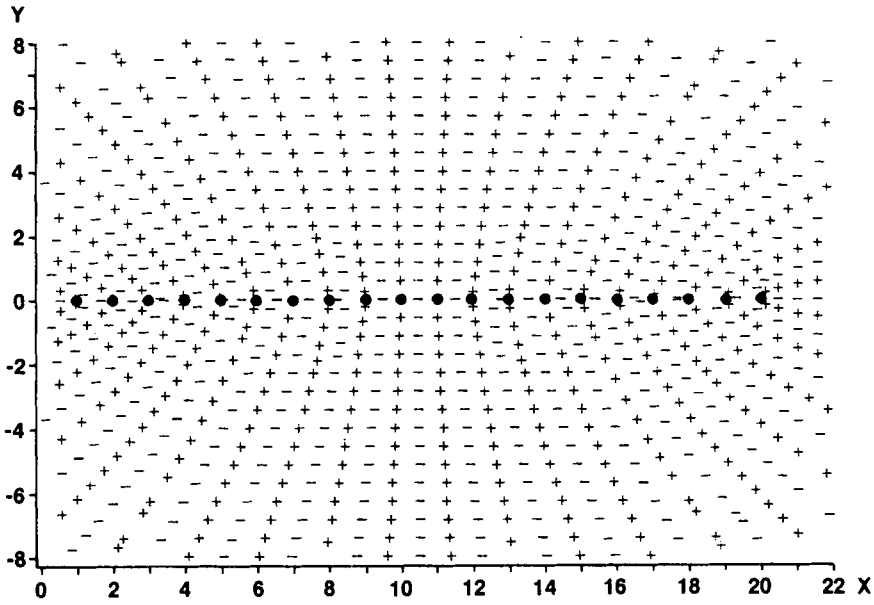

Fig. 7. The structure of 'Wilkinson's polynomial' $P = \prod_{i=1}^{20}(z - i)$. The graphs were produced by an IBM 7372 plotter from data points generated by the Main Algorithm (Appendix A). The + are tracepoints of the r-arcs, the − tracepoints of the i-arcs. The zeros are indicated by ●. The structure of a real polynomial is symmetric relative to the x-axis which is an i-branch. In this case there is an additional line of symmetry $x = 10.5$, which is also an i-branch. There are no branch regions; the function is univalent in each region bounded by r- and i-arcs.

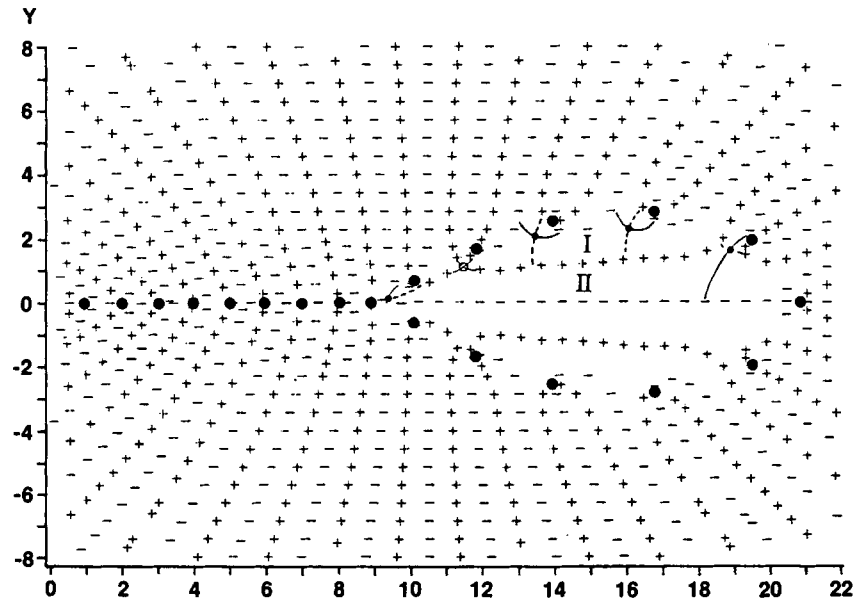

Fig. 8. The structure of the perturbed 'Wilkinson's polynomial' $P = 10^{-7}z^{19} + \prod_{i=1}^{20}(z - i)$. In each halfplane there occurs a branch point of r-arcs, indicated (by hand) by ○. Two branch regions of order 3 (in each halfplane) are discerned, indicated by I and II. On the basis of Corollary 1 the approximate location of the zeros of f' in I and II is sketched. The remaining zeros of f' are branch points.

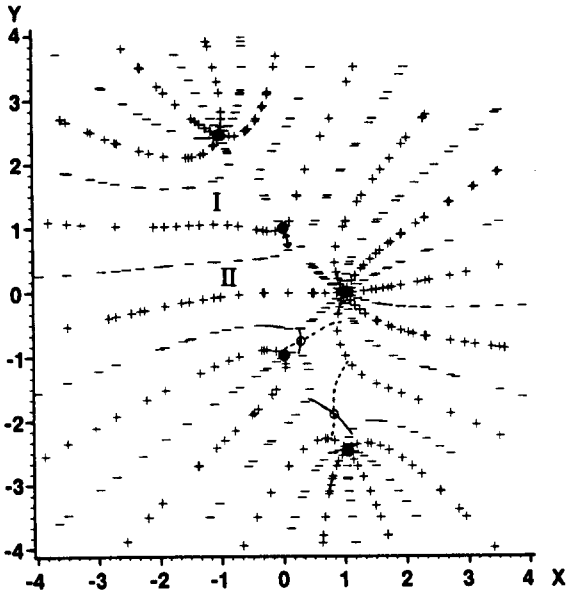

Fig. 9. The structure of a ninth degree complex polynomial $P=(z-1)^3(z^2+1)(z^2+5+5\mathrm{i})^2$. There are 2 branch region of order 2, indicated by I and II. This is an example in which the tracing is 'incomplete'. The arc indicated by $\leftrightarrow$ leading to $z=\mathrm{i}$ has not been traced. This is complemented by a doubly traced arc to $z=1$. In the third branch region, which has order 3, the 2 zeros of f' have been sketched.